2024 IEEE Latin-American Conference on Communications (LATINCOM) | 979-8-3315-2111-0/24/$31.00 ©2024 IEEE | DOI: 10.1109/LATINCOM62985.2024.10770662

Design and Implementation of a Low-Cost VLC Photovoltaic Panel-Based Receiver with off-the-Shelf Components

Agustín González-Uriarte
Department of Electrical Engineering
University of Chile
Santiago, Chile
agustin.gonzalez@ing.uchile.cl

Cesar Azurdia
Department of Electrical Engineering
University of Chile
Santiago, Chile
cazurdia@ing.uchile.cl

Diego Torreblanca
Department of Electrical Engineering
University of Chile
Santiago, Chile
diego.torreblanca@ing.uchile.cl

Pablo Palacios-Jativa
Esc. de Informatica y Telecomunicaciones
Universidad Diego Portales
Santiago, Chile
pablo.palacios@mail.udp.cl

David Zabala-Blanco
Department of Computing and Industries
Universidad Catolica del Maule
Talca, Chile
dzabala@ucm.cl

***Abstract*—This document introduces the design, implementation and evaluation of a functional visible light communication (VLC) system comprising a transmitter and receiver designed for use in a simultaneous lightwave information and power transfer (SLIPT) scenario, utilizing a photovoltaic panel. The circuit was made with low-cost off-the-shelf components, can be powered by a battery, is capable of enhancing the bandwidth of the photovoltaic panel, and is made as a proof of concept that inexpensive VLC systems are feasible. The system was shown to operate effectively in an indoor setting, where the existing lighting fixtures included an AC component with a frequency of 100 Hz, achieving a baud rate of 4.8 kBd over a distance of 60 cm between the transmitter and the receiver. The distance achieved could be useful for IoT devices that are near a light source but are unable to receive information via cable or other types of wireless technology.**

***Index Terms*—Low-cost systems, photovoltaic panel, SLIPT, VLC.**

I. Introduction

Current wireless technologies, including Wi-Fi, 4G, 5G, B5G, and LPWAN, among others, rely on radio frequencies (RF) to transmit information. As a result of the overwhelming number of technologies that use RF for communication, the electromagnetic spectrum has become congested, particularly at frequencies below 6 GHz [1]. This necessitates the use of frequencies in higher frequency bands or attempting to reuse existing frequency bands. An example of the latter is Narrowband IoT (NB-IoT) which improves the efficiency of the spectrum [2], and examples of the former are milimeter wave (mmWave), which functions in frequencies from 30 to 300 GHz [3], and optical wireless communications (OWCs) which function in frequencies of the order of THz [4].

A subset of OWCs is visible light communication (VLCs), which uses visible light as a wireless medium to transmit information [5]. In VLC systems, a light emitting diode (LED), an array of LEDs, or lasers are commonly used as transmitters while photodetectors (PDs) and other types of optical detectors are commonly used as receivers [1].

VLC systems that achieve data rates suitable for internet of things (IoT) applications typically employ photodiodes as optical receivers [1]; nevertheless, recently, photovoltaic (PV) panels have been tested as optical receivers in IoT-aimed VLC systems [4]. Compared to photodiodes, PV panels have the advantage of being able to harvest energy and receive information, and have been proven to reach data rates up to Gbps [4]. However, PV panels commonly used in the literature are expensive or specialized, making them difficult to acquire, especially on a tight budget [4].

This difficulty creates an elevated entry barrier for researchers, who might be budget-constrained, and industries that are not willing to invest their capital in a new technology, delaying the development and popularization of VLC-based IoT devices. Thus, this document introduces a functional low-cost IoT-oriented VLC system and describes its design, implementation, and evaluation.

The system is designed with the goal of being used in a simultaneous lightwave information and power transfer (SLIPT) [6] context; therefore, the optical detector of the receiver's circuit is a low-cost off-the-shelf PV panel, and the circuit components are also easy to acquire and inexpensive. In addition, the circuit enhances the bandwidth of the PV panel and can be powered with a battery.

The remainder of the paper is organized as follows: Section II introduces relevant information on PV panels and contextualizes the current state of the art. Section III details how the proposed VLC system was implemented, while Section IV discusses the performance of the system. Finally, Section V concludes and summarizes the work to come.

II. Related Work

Multiple studies [4] have been conducted on the capabilities of PV panels that serve as receivers in a VLC system. These studies have shown that data rates ranging from 2 kbit/s to 1041 Mbit/s are possible with distances between transmitter and receiver varying between 10 cm and 2 m, being the most common distance 30±10 cm.

The studies mentioned in [4] experimented with PV panels mostly under indoor conditions and used different types of PV panel, such as monocrystalline Si, polycrystalline Si, GaAs, amorphous Silicon (α-Si), Perovskite, and Organic PV (OPV) cells. In particular, GaAs cells have been shown to be able to achieve higher data rates, but OPV and perovskite cells have shown superior performance when used in SLIPT systems [4].

Top-performing systems often use specialized photovoltaic panels such as GaAs, OPV, or perovskite, and employ lasers or high-power LEDs as transmitters. These varieties of PV panels are preferred because of their inherent high bandwidth. In contrast, other types of PV panels, such as Poly-Si and Mono-Si, typically exhibit a lower bandwidth [4]. However, studies have shown that their bandwidth can be enhanced using various methods [7], [8].

A. Bandwidth of a PV panel

As in all communication systems, the bandwidth of the receiver is a big factor in the maximum achievable data rate, this makes analyzing the bandwidth of PV panels an important factor. As stated previously, the bandwidth of a PV panel depends on its type; in [4] it is shown that GaAs PV panels can have a bandwidth of more than 20 MHz, while silicon-based PV panels may have a bandwidth between 10 and 350 kHz. This makes it desirable to use GaAs PV panels.

Although GaAs PV panels have the highest inherent bandwidth, it is feasible to use other types of PV panels for communication, in [9] the authors proposed a circuit model for a PV panel when used in communication (AC signals), the circuit model is shown in Fig. 1 and when looking at the terminals from top to bottom, the voltage behavior is of a low-pass filter, where the constant RC is defined by the capacitor and resistors in parallel ($R = R1 \parallel R2$), as demonstrated in [10].

It is possible to observe that the bandwidth of the PV panel can be manipulated using a low value resistor as the load because the equivalent resistance of the lowpass RC filter would be lower [$R = R1 \parallel R2 \parallel (R3 + R_{\text{load}})$], causing the cutoff frequency to increase due to the following relation

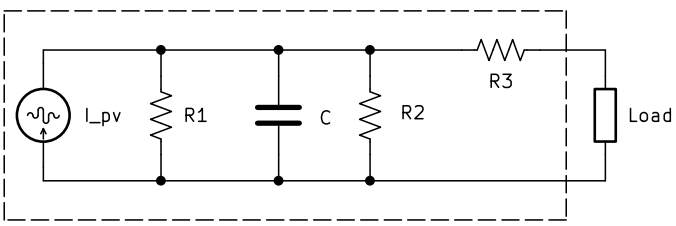

Fig. 1. Circuit model of a PV panel for AC signals.

$$f_{\text{cut-off}} = \frac{1}{2\pi RC}, \tag{1}$$

allowing for an increase in its bandwidth when desired. This behavior was demonstrated in [7] where the authors connected a load of 220 Ω to a PV panel of unknown type and increased its bandwidth from 3.5 kHz to 10 kHz. However, at the same time the amplitude voltage at the output decreased from 600 mV to 45 mV, negatively affecting the possibility of simultaneous EH.

B. Methods for Energy Harvesting

Different methods have been devised to harvest energy using PV panels when used in a SLIPT context, in [11] the authors propose three distinct receiver architectures for SLIPT, which they consider to be efficient:

1) Time Switching (TS) Receiver: This method implements two independent and unconnected circuits, one is used solely for EH and the other only for receiving information. To be able to do both jobs, the receiver switches between the circuits, harvesting energy for θT time and receiving information for $(1-\theta)T$ time, where $\theta \in [0,1]$ and T is an arbitrary unit of time. Since the circuit cannot harvest energy and receive information simultaneously, the parameter θ gains relevance since it dictates which characteristic is favored.

2) Signal Component Separation Receiver: In this method, the PV panel is connected to a splitter that separates the AC and DC signals, routing the DC voltage to the EH portion of the system and forwarding the AC signal to the portion of the system that receives information. This method may achieve a higher efficiency than TS due to carrying out communication and EH in parallel, instead of taking turns.

3) Photoelectric Converter Grouping Receiver: When the receiver circuit is composed of more than one PV panel, EH and information receiving can be done in parallel by grouping the PV panels into 2 groups, the first group is dedicated solely to EH, and the second only receives information. The groups are not definitive and may be changed during runtime to favor EH or communication, via the use of a switching key that the receiver could control. It is analogous to TS but without a set-switching period.

C. Current Implementations of Communication Receivers suitable for SLIPT Systems

Multiple SLIPT systems with PV panels have been designed and tested for communication purposes, varying the type of transmitter, modulation, and signal processor used to decode the information.

In Table I, different implementations of a VLC receiver with PV panels are shown, as well as the type of PV panel and modulation they used, the data rate and distance achieved, and if it is fully low-cost. All of these implementations use a low-cost PV panel as a receiver; however, an implementation is marked as fully low-cost if all components in the receiver, including the signal processor, are low-cost.

Table I shows that the systems achieve higher data rates when using more complex modulations, such as 16-QAM and

TABLE I
COMPARISON OF DIFFERENT IMPLEMENTATIONS IN THE LITERATURE

Ref.	PV Panel	Modulation	Data Rate	Distance [cm]	Fully Low-Cost
[7]	und§	OOK	38.40 Kb/s*	20	Yes
[12]	α-Si	PAM-4	01.25 Mb/s	15	No
[13]	poly-Si	OOK	01.50 Mb/s	100	No
[14]	und§-Si	16-QAM	15.03 Mb/s	200	No
[8]	mono-Si	DMT	17.05 Mb/s	10	No

∗ the original value was transformed to equivalent bits per second.
§ undisclosed.

DMT; nevertheless, data rates over 1 Mbps are achieved when using simpler modulations such as PAM-4 with pre-distortion [14] or On-Off Keying (OOK) in certain cases [13].

At the same time, in the systems shown, the distance achieved is not related to the data rate they accomplish. Usually, the type of signal decoder used dictates how complex the modulation or encoding can be, the theoretical maximum transmission speed, and, sometimes, the transmission distance due to hardware specifications such as CPU frequency, ADC sensitivity, and maximum sampling rate.

In the case of the systems shown in Table I, the receiver's most typical type of signal decoder is an oscilloscope with high processing power [8], [12], [13], [14], causing them not to be fully low-cost. However, the system in [7] is fully low-cost, because it uses an Arduino Uno to decode the received information, but the system's bit error rate (BER) does not satisfy the 7% forward-error-correction threshold and cannot be considered error-free [15].

III. Design Methodology and Experimental Setup

With the SLIPT system objectives defined, the communication functionality of the system was first designed and implemented, while the energy harvesting capability was decided to be left for future work.

To keep the system low-cost and off-the-shelf, the components acquired to build the system were: a battery powered emergency light composed of an array of LEDs, 2 WeMos D1 Mini DevBoards with an ESP8266 CPU, a 6V 11 by 6 cm polycrystalline silicon PV panel with a rating of 1W, multiple single supply OPAMPS (MCP6022), and other passive electronic components. The emergency light was modified to be powered externally, eliminating the need for batteries.

A. Analysis of theoretical maximum data-rate

To ensure a useful data rate for IoT applications, the communication capabilities of the components were analyzed, specifically the maximum sample rate of the ESP8266, the bandwidth of the emergency light, and the bandwidth of the PV panel.

The sampling rate of the ESP8266 is limited by its 80 MHz internal clock [16] and the software developed to receive and send information; for this an external library was used that implemented Manchester encoding and worked with rates up to 4.8 kBd when used with the ESP8266. Manchester encoding was chosen for the implementation due to its low complexity, OOK compatibility, and because its status as an official modulation for VLC in the IEEE 802.15.7 standard [17]. The Manchester library implemented an interrupt function triggered by a timer, which sampled the voltage on a pin, and checked if it corresponded to valid information.

To define a maximum sample rate, the time it took for the function to run was determined, for this the sampling function was modified to measure the time when the function entered and just before it exited, saving the time difference. This time difference indicated that the function took about 1.6 μs to run while receiving information, which implied that the ESP8266 could sample one digital pin with a maximum switching frequency of a bit more than 300 kHz due to the sampling theorem.

Although a theoretical value was reached, the maximum sampling rate was defined conservatively as 200 kHz because the CPU will also be in charge of carrying out other tasks, such as interacting with peripherals. The possibility of using more than one ESP8266 was not analyzed to try to keep the receiver low power.

The LED light was analyzed, and its bandwidth did not impose restrictions harsher than the one imposed by the ESP8266. On the other hand, when analyzing the bandwidth of the PV panel, it was found to have a 3 dB bandwidth of around

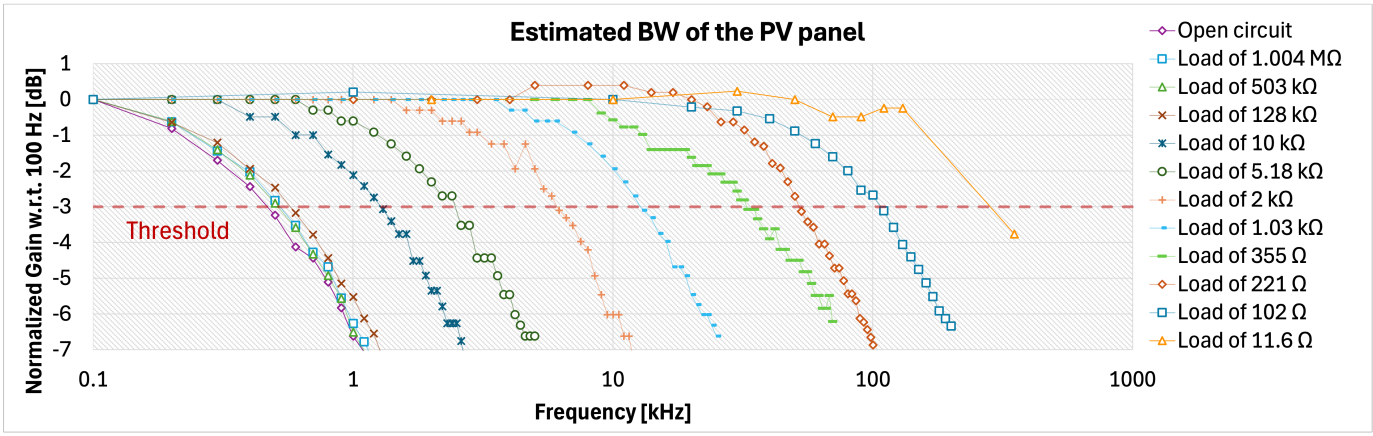

Fig. 2. Gain of the Poly-Si PV panel for different resistive loads when varying frequency.

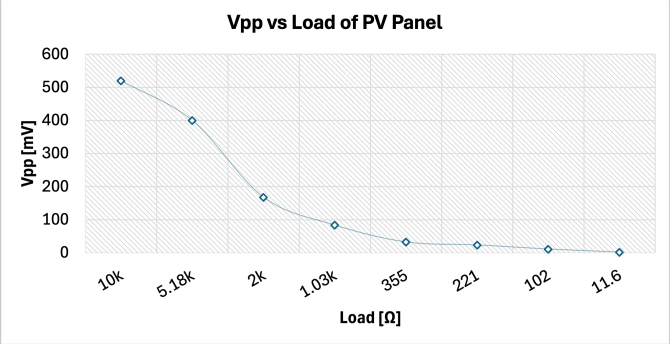

Fig. 3. Peak-to-peak voltage of the sinusoidal signal delivered by the PV panel for different loads.

500 Hz, imposing a very harsh restriction on the maximum data rate.

Since it was demonstrated in the literature that the bandwidth of a PV panel could be increased by connecting a resistive load to its terminal, various loads of different resistance were connected to the PV panel and its bandwidth was estimated using an AWG SIGLENT SDG2122 and a Tektronix TBS 1000C oscilloscope. The AWG sent sinusoidal signals of different frequencies using the LED light, and the power delivered by the PV panel was saved for the different loads and frequencies. The test was conducted in the dark to avoid interference from other light sources. The data collected is shown in Fig. 2 where the gain is normalized with respect to the power obtained when sending a signal of 100 Hz.

From Fig. 2, it is possible to observe that for loads greater than or equal to 128 kΩ the bandwidth remains close to 500 Hz, but when the load is further reduced, it increases to more than 1 kHz when using a load of 10 kΩ, and is close to 300 kHz when the load is 11.6 Ω. However, a small load value causes the PV panel voltage to decrease as shown in Fig. 3, where the peak-to-peak voltage of the received signal is shown versus the load connected to the PV panel terminals for loads equal to or lower than 10 kΩ since at that point the bandwidth starts to increase.

This confirms the trade-off between the increase in the bandwidth of the PV panel and the voltage it can deliver, and consequently, the achievable SNR. Although there are algorithms that optimize the trade-off between the energy harvested and the enhancement of bandwidth [18], a simple approach to define the load is used.

For the implemented system, it was decided that a load of 220 Ω was to be connected to the terminals of the PV panel, so that the PV panel could achieve a 3 dB bandwidth of 50 kHz and because a receiver circuit could amplify the delivered tens of milliVolts as long as the SNR was adequate. With the components analyzed, a theoretical rate of 50 kBd could be achieved, which is enough for small IoT devices.

B. Implementation details

A block diagram of the transmitter circuit is shown in Fig. 4, the MCU (WeMos D1 mini, ESP8266) controls the LED light by activating or deactivating an NPN transistor. The current

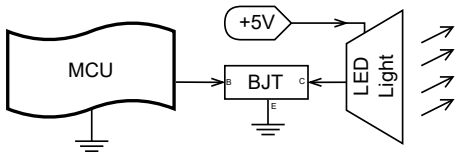

Fig. 4. Block diagram of the implemented transmitter circuit. The MCU is connected via a pin to the base of the BJT, while the negative terminal of the LED light is connected to the collector of the BJT. The emitter of the BJT is connected to ground, and the positive terminal of the LED to a 5V power supply.

that flows through the LED comes from an external 5V-2A power supply.

The block diagram of the receiver circuit is shown in Fig. 5, it is composed of the PV panel with a load of 220 Ω followed by a notch filter with a rejection frequency of 100 Hz, which is connected to a non-inverting amplifier, and finally a data slicer takes the previous amplifier signal and amplifies only the frequency components that are above 159 Hz. The output of the data slicer is then fed to a digital pin of the MCU (WeMos D1 mini), where the value is read by the software and processed.

The notch filter is configured for 100 Hz because the light fixtures where the system is tested have AC components of frequency 100 Hz, so by removing the signal at that frequency the SNR of the VLC signal is increased. This design choice causes the circuit to have trouble working in scenarios with different indoor lightning conditions, so in cases like that another type of filter should be used.

All components in the circuit are powered by the 3.3 V output of the WeMos D1 mini and the OPAMPS used are configured in a single supply mode, so they can be powered by a single battery.

The final setup is shown in Fig. 6, which was used to test the receiver. On the left is the transmitter composed of the transmitter circuit and LED light, and on the right is the receiver composed of the PV panel and the receiver circuit. The transmitter and receiver are 60 cm apart from each other and have line of sight (LOS).

Both WeMos D1 Mini were connected to the computer shown in the photo, which was capable of communicating with each MCU separately via a serial monitor. To send

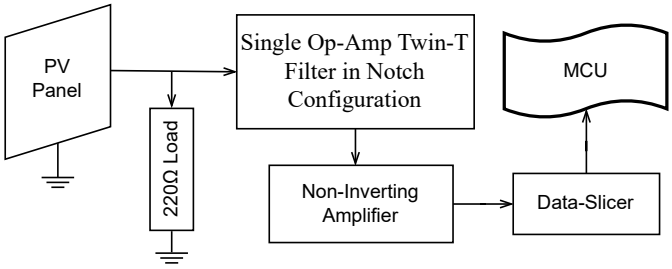

Fig. 5. Block diagram of the implemented receiver circuit. The positive terminal of the PV panel is connected to the BW-enhancer-220Ω load and the input of the notch filter. The filtered signal is then amplified, sliced to obtain valid logic-level voltages, and fed to the MCU.

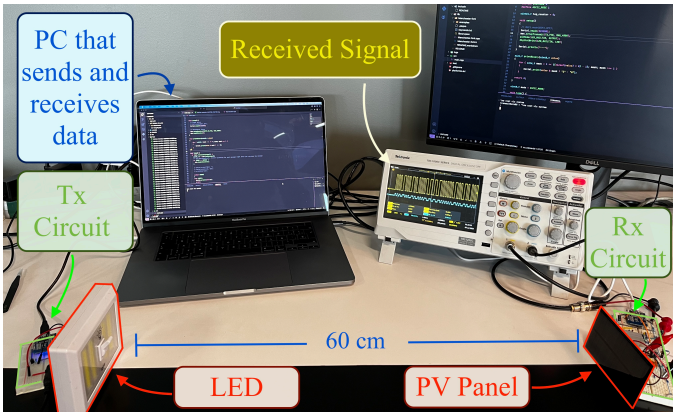

Fig. 6. Tested VLC setup. On the left is the transmitter with its circuit, and on the right is the PV Panel and the receiver circuit. Both circuits are communicate with the PC in the middle, and the oscilloscope is connected to the receiver's circuit. The received signal – in yellow – is the one shown in Fig. 7.

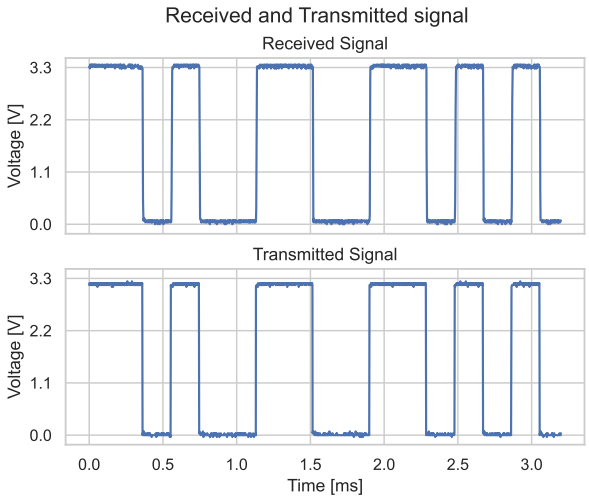

Fig. 7. Received and transmitted signal with manchester encoding at 4.8 kBd.

data, text had to be entered into the serial monitor connected to the transmitter, which converted the text into bytes, and then the receiver printed the bytes it received on its serial monitor. Between the receiver circuit and the computer was an oscilloscope connected to both the PV panel (blue signal) and the data slicer output (yellow signal).

The implemented setup was tested with the indoor lights on using a baud rate of 4.8 kBd, the maximum available baud rate for the ESP8266 in the Manchester encoding library, maintaining the aforementioned distance between the transmitter and the receiver.

IV. Results and Discussion

An excerpt of the received and transmitted signal after transmitting a random byte string can be seen in Fig. 7, the baud rate used was 4.8 kBd, the highest rate available for the ESP8266, the distance between the transmitter and the receiver was 60 cm, and the system was placed in an indoor environment as shown in Fig. 6.

From Fig. 7 it is possible to observe that the received signal is almost identical to the sent signal, with the sole exception that the rise time of the received signal is a bit longer than the sent signal. This difference is visible around the 2.5 ms mark, where the transmitted signal changes from low to high just before the 2.5 ms mark, while the received signal reaches the high state just at the 2.5 ms mark. This increased rise time may not be a problem for the used baud rate but could be a problem for higher rates.

After transmitting hundreds of bytes, the system was confirmed to be working error-free for a distance of 60 cm, it was verified by comparing the received bytes versus the transmitted. This outcome indicates that the WeMos D1 Mini is capable of decoding the received information. Furthermore, the result demonstrates that the VLC receiver worked as expected in indoor conditions, achieving distances between the transmitter and the receiver that could be useful for IoT devices that are near a light source but cannot receive information via wired methods or other types of wireless technologies.

The distance achieved by the system was due to the emitted power of the LED used and the sensitivity of the receiver circuit, where the notch filter introduces power losses that the amplifier is not capable of compensating for. To extend the transmission distance, the sensitivity of the receiver circuit or the emitted power of the LED should be increased.

Due to the receiver circuit rise time being different from the transmitter rise time, a second test was conducted focusing only on the receiving circuit and not on the communication capabilities of the whole system. For this, the setup conditions of the first test were kept with the difference that a square wave signal with a frequency of 10 kHz, duty cycle of 50%, amplitude of 3.3 V and offset of 1.65 V was sent using an AWG SIGLENT SDF2122. The signal generated by the AWG simulates a signal that could be sent by the WeMos D1 mini when using a baud rate of 20 kBd.

Fig. 8 shows the transmitted signal, the AC component of the signal delivered by the PV panel, and the signal delivered by the full receiver circuit. In the top plot, it can be observed that the PV panel responds well to the transitions of the transmitted signal, and the low-pass filter behavior of the PV panel can be observed in the rise and fall times of the delivered signal. Similarly, in the bottom plot the signal that would go to the WeMos D1 mini is observed, it also has an increased rise and fall time compared with the transmitted signal, which is congruent with the behavior highlighted on the first test. This increased rise and fall times caused the duty cycle of the received signal to be different from 50%, which could be a problem at the time of decoding the information. However, due to software limitations, it is not possible to test the equivalent baud rate in the system.

The increase in rise and fall times for signals with an equivalent baud rate of 20 kBd indicates that the implemented circuit is capable of guaranteeing a baud rate of 4800 Bd when using a PV panel as a receiver, which is sufficient for certain IoT applications. However, if higher rates are needed, changes to the circuit or another circuit may be necessary.

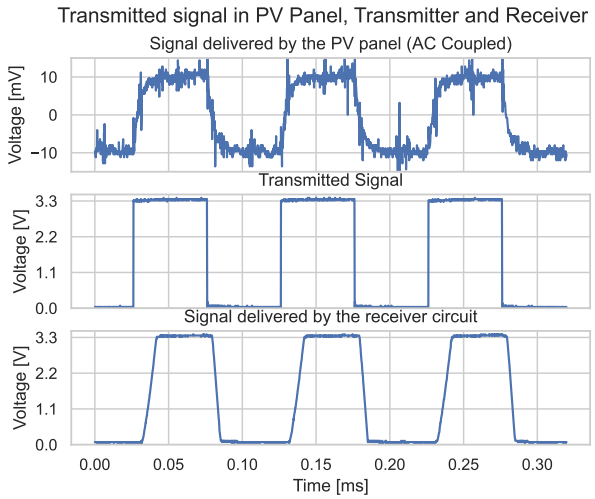

Fig. 8. 20 kBd signal in different points of the system.

It is also possible to observe in Fig. 8 that the voltage of the AC component delivered by the PV panel is around 20 mV peak to peak, which is consistent with what was discussed in Section III, while the voltage of the signal delivered by the receiver circuit varies between 0 and 3.3 V, demonstrating that the designed receiver circuit can operate with low voltage variations coming from the PV panel.

Compared to the systems shown in Table I – except [7] – the implemented system is fully low-cost, making it a more viable alternative for budget-constrained entities interested in this technology. Meanwhile, compared to [7], the system achieves error-free communication and a longer transmission distance by using an array of LEDs instead of a blue LED. In addition, the trade-off between energy harvesting and bandwidth is analyzed in this document, facilitating its use in SLIPT systems.

V. Conclusion and Future Work

In this work, a working VLC receiver and transmitter to be used in a SLIPT system were implemented using low-cost off-the-shelf components. The system was able to increase the bandwidth of a PV panel from 500 Hz to 50 kHz and achieve error-free baud rates of 4.8 kBd at a distance between transmitter and receiver of 60 cm. Furthermore, the performance of the system makes it suitable for IoT applications that need low data rates and are unable to communicate using conventional technologies.

While a VLC circuit utilizing a PV panel is operational, the creation and deployment of a suitable energy harvesting circuit are deferred for future work to accomplish a SLIPT system. Given the impact of the installed VLC receiver on the PV panel's peak-to-peak voltage, employing a time-switching approach for energy harvesting might prove advantageous.

Acknowledgment

This work was supported by ANID/FONDECYT Regular No. 1211132, ANID/FONDECYT Iniciación No. 11240799 and Departamento de Ingeniería Eléctrica de la Universidad de Chile.

References

[1] A. Celik, I. Romdhane, G. Kaddoum, and A. M. Eltawil, "A Top-Down Survey on Optical Wireless Communications for the Internet of Things," *IEEE Communications Surveys & Tutorials*, vol. 25, no. 1, pp. 1–45, 2023.

[2] "Narrowband – Internet of Things (NB-IoT) — gsma.com," https://www.gsma.com/solutions-and-impact/technologies/internet-of-things/narrow-band-internet-of-things-nb-iot/, [Accessed 06-07-2024].

[3] A. Nordrum and K. Clark, "5G Bytes: Millimeter Waves Explained — spectrum.ieee.org," https://spectrum.ieee.org/5g-bytes-millimeter-waves-explained, may 2017, [Accessed 06-07-2024].

[4] J. Bouclé, D. Ribeiro Dos Santos, and A. Julien-Vergonjanne, "Doing More with Ambient Light: Harvesting Indoor Energy and Data Using Emerging Solar Cells," *Solar*, vol. 3, no. 1, pp. 161–183, 2023.

[5] S. Vappangi, V. V. Mani, and M. Sellathurai, *Visible light communication*. Boca Raton: CRC Press, Jul. 2021.

[6] P. D. Diamantoulakis, G. K. Karagiannidis, and Z. Ding, "Simultaneous Lightwave Information and Power Transfer (SLIPT)," *IEEE Transactions on Green Communications and Networking*, vol. 2, no. 3, pp. 764–773, 2018.

[7] S. Valencia Lozano, R. A. Martínez Ciro, and F. E. López Giraldo, "Evaluation of an AGC for a Solar Panel as a Receiver in a VLC System Applied to Access Control," *IEEE Latin America Transactions*, vol. 22, no. 5, pp. 428–434, 2024.

[8] W.-H. Shin, S.-H. Yang, D.-H. Kwon, and S.-K. Han, "Self-reverse-biased solar panel optical receiver for simultaneous visible light communication and energy harvesting," *Opt. Express*, vol. 24, no. 22, pp. A1300–A1305, Oct 2016.

[9] Z. Wang, D. Tsonev, S. Videv, and H. Haas, "On the Design of a Solar-Panel Receiver for Optical Wireless Communications With Simultaneous Energy Harvesting," *IEEE Journal on Selected Areas in Communications*, vol. 33, no. 8, pp. 1612–1623, 2015.

[10] S. Kadirvelu, W. D. Leon-Salas, X. Fan, J. Kim, B. Peleato, S. Mohammadi, and B. Vijayalakshmi, "A Circuit for Simultaneous Reception of Data and Power Using a Solar Cell," *IEEE Transactions on Green Communications and Networking*, vol. 5, no. 4, pp. 2065–2075, 2021.

[11] G. Pan, P. D. Diamantoulakis, Z. Ma, Z. Ding, and G. K. Karagiannidis, "Simultaneous Lightwave Information and Power Transfer: Policies, Techniques, and Future Directions," *IEEE Access*, vol. 7, pp. 28 250–28 257, 2019.

[12] H. Y. Wang, J. T. Wu, C. W. Chow, Y. Liu, C. H. Yeh, X. L. Liao, K. H. Lin, W. L. Wu, and Y. Y. Chen, "Using pre-distorted PAM-4 signal and parallel resistance circuit to enhance the passive solar cell based visible light communication," *Optics Communications*, vol. 407, pp. 245–249, 1 2018.

[13] Rahul, A. Mitra, A. Srivastava, V. A. Bohara, and D. Solanki, "Experimental Validation of Optical Wireless Receiver using Solar Panel with Bandwidth Enhancement Circuit," in *IEEE Vehicular Technology Conference*, vol. 2022-June. Institute of Electrical and Electronics Engineers Inc., 2022.

[14] R. Sarwar, B. Sun, M. Kong, T. Ali, C. Yu, B. Cong, and J. Xu, "Visible light communication using a solar-panel receiver," *ICOCN 2017 - 16th International Conference on Optical Communications and Networks*, vol. 2017-January, pp. 1–3, 11 2017.

[15] E. Agrell and M. Secondini, "Information-Theoretic Tools for Optical Communications Engineers," *31st Annual Conference of the IEEE Photonics Society, IPC 2018*, 11 2018.

[16] *Wireless SoC - Datasheet*, Espressif Systems, 2023, ver. 7.0.

[17] S. Rajagopal, R. D. Roberts, and S. K. Lim, "IEEE 802.15.7 visible light communication: Modulation schemes and dimming support," *IEEE Communications Magazine*, vol. 50, pp. 72–82, 3 2012.

[18] S. Sepehrvand, L. N. Theagarajan, and S. Hranilovic, "Rate-power tradeoff in simultaneous lightwave information and power transfer systems," *IEEE Communications Letters*, vol. 25, pp. 1249–1253, 4 2021.